

GRAPH BASED MAPPING OF URBAN STRUCTURE TYPES FROM HIGH RESOLUTION SATELLITE IMAGE OBJECTS

I. Walde, S. Hese, C. Schmullius

Friedrich-Schiller-University Jena, Institute of Geography, Earth Observation,
Graduate School on Image Processing and Image Interpretation
(irene.walde, soeren.hese, c.schmullius)@uni-jena.de

KEY WORDS: Land Use, Land Cover, Urban, Planning, High resolution, Structure, Value-added

ABSTRACT:

Due to the ongoing urbanization (e.g. urban sprawl) the demand for frequent updates of urban land use classes for monitoring, controlling and modeling purposes is increasing. The derivation of urban land use (LU) from satellite images is an added value that can not be achieved directly from the data itself. Distinguishable structures and patterns are described using thematic, morphological, topological and spatial properties forming specific relations of land cover classes. The objective of this work is to formalize those properties and relations within a graph based concept to model a specific urban land use type by identifying typical spatial arrangements. The study area is Rostock, a German city at the Baltic Sea with more than 200.000 inhabitants. For first analysis cadastral building polygons and building objects derived from high resolution Quickbird data and LiDAR building heights are used. Nodes describing a certain urban object and edges representing a relation of the object are the components of a graph. At first the distribution of the cadastral building objects is investigated to generate meaningful Euclidean distance ranges. Graphs of the distance ranges are generated and compared using graph measures that evaluate the compactness and connectivity of the graph, like alpha-, beta-, gamma-index and the clustering coefficient. Afterwards the appliance of the distance ranges on building polygons derived from segmentation algorithms of Quickbird images is tested. The results show that the spatial relation of distance is a reliable indicator for distinguishing urban LU-categories. The separability of LU-classes should be improved by combining significant properties of land cover classes and graph indices to a LU-signature.

KURZFASSUNG:

Aufgrund der fortschreitenden Verstädterung (Suburbanisierung/Zersiedelung) wächst der Bedarf an regelmäßiger Aktualisierung urbaner Landnutzungsklassen für Modellierungs-, Überwachungs- und Kontrollzwecke. Die Ableitung urbaner Landnutzung aus hochauflösenden Satellitenbildern stellt einen Mehrwert dar, der nicht direkt aus den Daten extrahiert werden kann. Erkennbare Strukturen und Muster werden mit Hilfe von thematischen, morphologischen, topologischen und räumlichen Eigenschaften und Beziehungen zwischen Landbedeckungsklassen verdeutlicht. Das Ziel des Projektes ist es diese Eigenschaften und Beziehungen in einem Graphen-Konzept umzusetzen, um urbane Objekte und deren räumliche Anordnung zu modellieren. Das Untersuchungsgebiet ist Rostock, eine deutsche Stadt an der Ostsee mit mehr als 200.000 Einwohnern. Für erste Untersuchungen wurden Gebäudepolygone aus der Automatisierten Liegenschaftskarte (ALK) und Gebäudeobjekte, abgeleitet aus Quickbird Satellitendaten und LiDAR Gebäudehöhen, verwendet. Knoten, die ein bestimmtes Stadtobjekt beschreiben und Kanten, welche die Beziehung der Objekte zueinander definieren, sind die Komponenten des Graphen. Die Verteilung der ALK-Gebäudepolygone wird untersucht, um signifikante euklidische Distanzbereiche zu erhalten. Mit Hilfe der Distanzbereiche werden Graphen erzeugt und spezifische Indikatoren verwendet, um die Graphen bzgl. Kompaktheit und Verbindungsgrad zu vergleichen. Anschließend wird die Übertragbarkeit der Distanzbereiche auf Gebäudeobjekte getestet, die auf Basis von Segmentierungsalgorithmen aus Quickbirddaten abgeleitet wurden. Die Ergebnisse zeigen, dass die räumliche Eigenschaft der Distanz ein verlässlicher Indikator für die Unterscheidung von urbanen Landnutzungskategorien ist. Die Trennbarkeit urbaner Landnutzungsklassen kann verbessert werden, indem man signifikante Eigenschaften der Landbedeckungsklassen und Graphenindikatoren zu einer Landnutzungssignatur kombiniert.

1 INTRODUCTION

Urban areas grow constantly and parts of them change in form, functionality, demographic structure and are damaged by natural disasters or human impacts like wars and rebuilt. The United Nations Habitat announced in their "State of the world's cities 2010/2011" that by 2030 more people of the world will live in cities than in rural areas (UN Habitat, 2011). Urbanization is the least reversible human dominated LU-type. The consequences range from land cover change to climate impacts, habitat loss or extinction of species and influence transportation development, energy demand or specific commercial markets (Seto et al., 2011). The European Environment Agency mentioned the main drivers in Europe as: population increase, rising living standards, improvement of quality of life, economic growth, globalization, policies

and regulations, low transport costs, availability of roads and others (European Environment Agency, 2010). Hence there is a need for urban LU-information for sustainable planning and development applications, for political decision making, monitoring of ecosystem changes, disaster management or analysis of quality of living. The urbanization process is inevitable but the awareness to handle, plan and manage urban growth sustainable, careful and ecology-minded should be pushed forward. According to Di Gregorio (2005) "Land Use is characterized by the arrangements, activities and inputs people undertake in a certain land cover type to produce change or maintain it." (Di Gregorio, 2005). Barnsley and Barr (1997) describe land use as "abstract concept – an amalgam of economic, social and cultural factors – one that is defined in terms of function rather than physical form.". So far urban land use is collected from surveying, mapping or digitizing,

population statistics or inquiries. These methods require high financial and personal investments, are time-consuming and therefore less actual. The benefits of an approach based on satellite images are the high temporal resolution, a constant coverage and an area wide availability. Urban land use is an added value that can be derived indirectly from urban land cover and its properties. Properties like building area, object shape, building height, neighborhood or imperviousness describe a certain area and create a distinguishable structure. A graph, as an abstract concept of real world phenomena, can store these properties as node- or edge-attributes and can emulate the structure of the LU-category. The paper will give a brief overview of related work, the study site and available datasets and a short digression into graph theory follows. In section 5 the data analysis starts with a description of the observed LU-classes. Afterwards the distribution of buildings is examined to derive distance ranges for analyzing the influence of distance when creating urban building graphs. Finally a first approach to transfer the graph based concept to buildings derived from satellite data is presented. The paper concludes with a summary of the results and suggests future work.

2 RELATED WORK

Graph theory is applicable to various disciplines and networks which illustrate issues in biology, geography, ecology or economics are ubiquitous. Image Processing is a field of application of graph theory which is not only related to remote sensing but also to medicine, informatics and others. It is worth to gain insight into those research fields when working with graph theory for structural analysis and classification approaches. Deuker et al (2009) used various graph indices for analyzing complex networks in human brains. Magnetoencephalography (MEG)-Images from brains in state of rest and solving memory exercises were compared. Therefore global graph indices (clustering coefficient, path length, small-worldness, assortativity, hierarchy etc.) were calculated on different frequency interval networks. These indices were classified into first (clustering coefficient, path length) and second order (small-worldness, assortativity, hierarchy) depending on how many graph properties are required to compute the index. Gunduz et al (2004) classified cancer cells in brains (glioma) in tissue images by topological properties. After using Euclidean distance and Waxman model for graph generation, various graph indices and artificial neural network (ANN) classification were accomplished. Three resulting classes for the cells were achieved: healthy, cancerous and inflamed.

Within remote sensing and geoinformatics applications a derivation of urban LU-classes based on graphs was established by Barnsley and Barr (1997). Their developed data model called XRAG (eXtended Relational Attribute Graph) exists of nodes, edges each with its properties, the land cover label, possibility of grouping and the probability of the assigned land cover class. Morphological, relational as well as spatial properties of land cover types were derived from topographic maps in raster format. Graphs based on spatial relations (adjacency, containment) were built and the node degrees of three residential areas of different decades and a hospital complex compared. Bauer and Steinnocher (2001) implemented rules for LU extraction within eCognition software (Benz et al., 2004) based on previous analysis in SAMS (Structural Analyzing and Mapping System), where XRAG is included. Investigating urban topological structures De Almeida et al (2007) used graph-search algorithms to describe the topological property of containment. Triangulated LiDAR data was used and the slope of the triangles calculated. A classification of flat and steep polygons followed. Finally depth-first search (DFS) and breadth-first search (BFS) algorithms in graph-

trees were compared. A graph clustering technique presented by Anders et al (1999) was used to infer higher level urban structures from detailed cadastral map data to allow a multi-scale map generation. Using a Delaunay triangulation (DT) a relative neighborhood graph (RNG) was generated. After the removal of outlier edges the local neighbor density was estimated from the mean distance of edges.

3 STUDY SITE AND DATASET

The study area is Rostock, a German Hanseatic city, situated along the Warnow river and at the Baltic Sea with more than 200.000 inhabitants and an area of circa 181 km². Vector data from the German automated real estate map (ALK) and a digital landscape model (DLM) of Rostock were beneficial to allocate training areas, to develop the method and to evaluate the outcome. The boundaries of the DLM dataset are classified relating to the LU-types (see Sec.5). A cloud-free Quickbird scene with a pan-sharpened spatial resolution of 60 cm from September 2009 is available (Figure 1). The Quickbird image data is corrected for atmospheric effects using ATCOR2 (Richter et al., 2006). Due to the fact that a topographic correction is not included in the Ortho Ready Standard Imagery product the CE90 (Circular Error with 90% level of confidence) is denoted as 23 m or higher, depending on terrain variability in the scene and the view angle (Cheng et al., 2003). Therefore the Quickbird scene is corrected by a projective transformation using 30 well distributed ground control points acquired from the cadastral building data and the digital elevation model (DEM) from LiDAR data. To obtain relative object heights (buildings and vegetation) a normalization (nDSM) of LiDAR data with a point density of two points per square meter collected in 2006 with the DEM is performed.



Figure 1: Quickbird satellite image with superimposed borders of Rostock (©DigitalGlobe, Inc., 2011)

For comparison purposes of the methods a segmentation of the satellite image and the nDSM is performed followed by an object based classification to extract the building land cover by Voltersen (2011). Therefore the mean nDSM height of 2 m is the first criterion. Afterwards the separation of buildings and trees is achieved by considering the Normalized Differenced Vegetation Index (NDVI).

4 GRAPH THEORY

In 1736 Euler abstracted the problem of the „Seven Bridges of Königsberg“ and proved that a round tour crossing every bridge only once is impossible. This abstraction was denoted as the initiation of a branch of mathematics called graph theory. Various applications e.g. routing algorithms, social and cognitive networks, technological networks, cell networks or ecological networks, infrastructure networks, flow models, minimal costs computation etc. emphasize the interdisciplinary character of graph theory. A graph comprises vertexes (nodes) and edges (links) (Caldarelli, 2007) and is defined by its adjacency matrix. The row and column-indices of this matrix stand for the vertexes while the binary entries represent the connection of the vertexes (1=connected, 0=not connected). Graph measures indicate structural characteristics of graphs. The beta index (1), defined by edges (e) over vertexes (v) is a measure for connectivity (Rodrigue et al., 2009).

$$\beta = \frac{e}{v} \quad (1)$$

The gamma index (2) is the quotient of the observed edges over the maximum possible number of edges. It ranges between 0 and 1, where 1 stands for a complete graph with no subgraphs.

$$\gamma = \frac{e}{3(v-2)} \quad (2)$$

The alpha index (4) indicates the redundancy of a graph and is defined by the ratio of observed cycles (meshes) over the maximum possible cycles. Its values vary between 0 and 1, while 1 stands for a fully connected graph. A cycle or mesh is a chain of edges with same start and end node and no edge is crossed more than once. The number of cycles (u) (3) is calculated from edges (e), vertexes (v) and the number of sub-graphs (p), which are subsets of a graph (Rodrigue et al., 2009, Stuttgart, 2011).

$$u = e - v + p \quad (3)$$

$$\alpha = \frac{u}{2v - 5} \quad (4)$$

More extensive graph indices could reveal structural differences between networks. The clustering coefficient, also named transitivity in social network research, reveals whether neighbors of a vertex are also adjacent to each other. It reveals cluster or communities with a similar degree of links. While the local clustering coefficient unveils the clustering of a specific node the global (5) indicates the probability of a graph that adjacent nodes are connected. Watts and Strogatz (1998) introduced the clustering coefficient for social networks. In Newman et al (2001) the clustering coefficient is defined as

$$C = \frac{3 \times \text{number of triangles on the graph}}{\text{number of connected triples of vertexes}} \quad (5)$$

A connected triple stands for a vertex which is connected to two other vertexes. Hence a complete triangle consists of three connected triples (Watts and Strogatz, 1998, Newman et al., 2001, Rodrigue, 2009).

5 DATA ANALYSIS

A goal of the project was to analyze the distance of neighboring buildings as a property that could reveal urban typology. Five meaningful urban LU-classes are defined in Table 1 delineating the typical German urban land use. Characteristics are adopted from Breuste et al (2001) or properties like imperviousness or green area index from Banzhaf and Höfer (2008). Building area index (BAI) and floor area index (FAI) are upper limits declared by the German Federal Land Utilization Ordinance (Bundesministerium der Justiz, n.d.). While the BAI is defined as the ratio of the building area over the parcel area, the FAI is the quotient of the floor area over the parcel area.

LU-class	Description
City center (1)	Dense multi-storied building type next to the street, narrow streets or alleys, small paved or vegetated courtyards, paved open areas, churches, city halls, very high imperviousness (70-90%), BAI=1, FAI=3
Residential single family houses (2)	low building density with detached 1- or 2-storied houses, uniform urban settlement up to individual shaped buildings, access to roads, garages, pools, terrace as paved areas, low to intermediate imperviousness, BAI= 0.2-0.6, FAI=0.4-1.2
Residential block buildings (3)	Large rectangular simple form buildings, regular alignment, more than 3 stories, low to intermediate imperviousness, green area index 25-80%
Industrial area (4)	large, multi-storied or low-rise buildings, extensive paved area for parking lots, often situated next to railroad lines, port facility or highways, isolated few or no vegetation areas, often no clear spatial structure, BAI=0.8, FAI=2.4, green area average 16%
Allotment (5)	Detached small sized buildings (hovels, arbors), low built up, low imperviousness, abundant vegetation, BAI=0.2, FAI=0.2, next to forest or green areas, used as buffer between railroad lines, high traffic-roads, industrial areas and residential buildings

Table 1: Urban land use classes

5.1 Analysis of ALK Building Polygons

For the following analysis the DLM-boundaries, which surround a square of streets, in the settlement areas of Rostock are used. Thereby industrial and allotment areas are extracted directly. Areas with appellation of harbor, dockyard, power station and water works are classified as industrial as well. The residential classes single, block and city center are assigned manually using the DLM-boundaries declared as general residential building area, area of mixed use and area with special functional embossing. Additionally boundaries with less than five buildings are disregarded due to insufficient significance. In Figure 2 the resulting DLM-boundaries with their allocation to the LU-classes are visualized. To establish distance ranges of buildings for the graph development it is essential to investigate the distribution of the buildings within each DLM-boundary. If the appearance of the buildings is rather clustered than random or dispersed,

the derivation of a mean distance value would not be meaningful and would not result in useful findings. The applied method for the investigation of the distribution is described in detail by Trauth (2010,p.221ff.). Therefore the buildings of the real estate map layers 11 and 84 (predominantly garden houses) are used and centroids are computed. A nearest neighbor criterion is applied, starting with the calculation of the mean nearest neighbor distance. The expected mean nearest neighbor required a value for the area under investigation. The area of the DLM-boundary is not reasonable because they could be greater than the occurrence of the buildings. At the city borders where no street limits the outside of the city a crossover to agricultural fields or woods is noticeable. Due to these circumstances the area of the convex hull of the buildings within each DLM-boundary is chosen. Afterwards the z-distribution (standard normal distribution) is computed using the standard error of the mean nearest-neighbor distance. At a significance level of 95% the z-distribution has its critical values of 1.96 and -1.96. This connotes that values below -1.96 leads to clustered distribution, values above 1.96 mean dispersed and values in between represent random distribution.

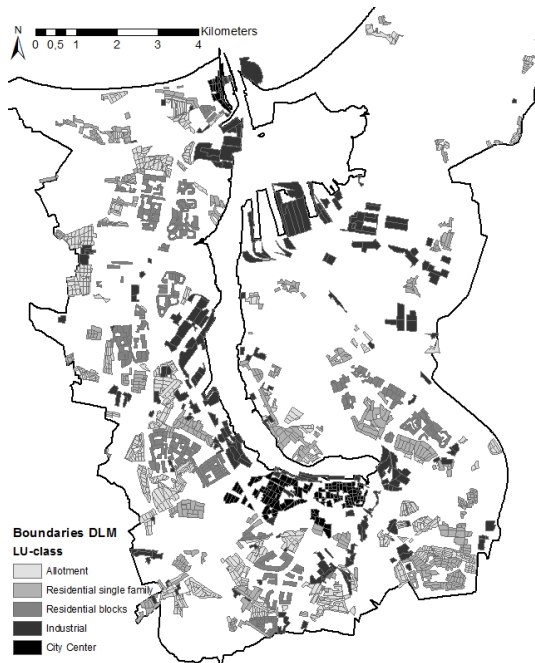


Figure 2: Boundaries of the digital landscape model of Rostock with assigned land use classes

In Table 2 the distribution of the buildings split by LU-class is summarized. A visual inspection of the clustered polygons shows that often a complex form of the DLM-boundaries is responsible for the clustered result. These outlier-polygons were removed from further analysis to ensure valid results.

LU-class	dispersed	random	clustered	Sum
city center	129	17	2	148
single family	383	42	5	430
block buildings	212	29	3	244
industrial	221	29	3	253
allotment	676	58	7	741

Table 2: Summary of amount of DLM-boundaries assigned to distribution category

In the next step a Delaunay triangulation (DT) of the building centroids per DLM-boundary is computed, which takes the spa-

tial relationship of neighborhood of buildings into account. The result is a planar graph per DLM-boundary where the mean edge length is calculated. In Table 3 the statistics of the mean distance values of the LU-classes is summarized. It reveals that the city center, residential single family houses and allotment areas often have similar spacing of buildings as well as that industrial and block building areas represent a group. Deduced from the median and the interquartile range two distance ranges are determined: 0-35 m and 35-85 m.

LU	Mean	SD	Median	Q1	Q3	IQR
1	24.48	8.52	22.98	18.47	27.91	9.44
2	26.64	8.37	25.46	21.36	30.50	9.14
3	55.29	26.41	54.70	37.60	72.96	35.36
4	70.09	42.59	59.56	44.04	79.87	35.83
5	29.53	11.07	26.27	22.91	32.92	10.01

Table 3: Summary of statistics of mean distance values split by LU-class (SD=Standard deviation, Q1=25th percentile, Q3=75th percentile, IQR=Interquartile range)

Two different graphs per DLM-boundary are built. Based on the DT the graphs are thinned out by values which are outside of the distance ranges. The geometric graph visualization of a residential single family house-area and an industrial area during the two distance ranges is shown in Figure 3.

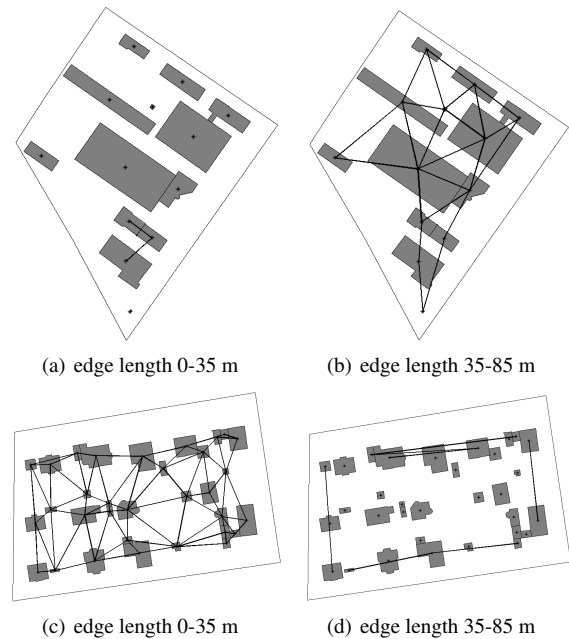


Figure 3: Planar graphs of cadastral building polygons (ALK): industrial area (a),(b); residential single family house-area (c),(d)

Looking at the two distance ranges the graph structure changed. E.g. in the industrial area the graph changes from a sparsely connected in the 0-35 m range to a multiple connected graph in the 35-85 m range. In the next step the graph measures described in section 4 are computed. Exemplary the box plots of the beta index and clustering coefficient are shown in Figure 4.

The beta index of single family houses, city center and allotment areas for the distance range 0-35 m showed extreme values as expected. The beta index values for the distance range 35-85 m are similar for all LU-classes. This is explained by the long edges at the border of the triangulation that occurred with the classes single family houses, city center and allotment areas, which also appears in Figure 3(d). The box plots of gamma and alpha index

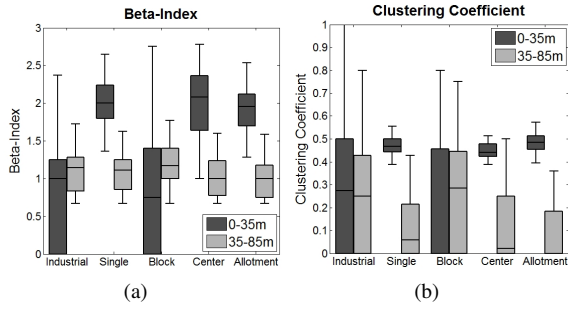


Figure 4: Box plots of beta index(a) and clustering coefficient(b) of planar graphs of cadastral building polygons (ALK)

are similar to the beta index plot. Due to their related algorithm basis the three measures strongly correlate in planar graphs. The box plot of the clustering coefficient shows a significant narrow interquartile range for single family houses, city center and allotment areas in the 0-35 m range while in the 35-85 m range a considerable descent is observed. The clustering value of industrial and block areas has a high variance with no significant changes between the distance ranges.

5.2 Analysis of Building Objects from the Quickbird Scene

These investigations of distance as a spatial relation between buildings are transferred to buildings derived from spatial high resolution satellite data. The same initial DLM-boundaries are used. As with the cadastral building polygons the boundaries with less than five buildings are disregarded. During distribution analysis we found that the amount of boundaries is noticeably smaller than with the cadastral building polygons. The explanation is that the polygons classified as buildings are merged when they have a building neighbor. This resulted for most of the city center boundaries that only one building is found per boundary and these boundary therefore were removed. Also in residential single family house areas a merging of neighboring buildings means a fusion of house and garage when these objects are located next to each other. The DT of the remaining LU-boundaries is calculated and the statistical analysis of the mean distance is computed and summarized in Table 4.

LU	Mean	SD	Median	Q1	Q3	IQR
1	52.01	11.66	48.58	43.85	61.01	17.17
2	48.23	13.29	45.30	38.84	54.61	15.77
3	74.63	30.02	70.75	50.56	91.11	40.55
4	89.50	40.24	79.58	62.94	105.76	42.82
5	40.47	15.64	36.60	30.65	45.74	15.09

Table 4: Statistics of mean distance of building land cover from satellite images after DT split by LU-class (SD=Standard deviation, Q1=25th percentile, Q3=75th percentile, IQR=Interquartile range)

The similar spacing of city center, residential single family houses and allotment areas still remains but the median distance of the buildings increased up to 25 m, due to the mentioned merging. The median of industrial and block building house areas increased by 10 to 15 m. The interquartile range go along with the observed increase of the median and is widened. Especially the IQR-value for the city center showed the highest raise. This leads to a new definition of the distance ranges for the graphs. Deduced from the median values and the IQRs the two distance ranges of 0-60 m and 40-150 m are determined with an overlap of 20 m. The two different graphs per DLM-boundary are built by thinning out the edges of the DT removing the values outside of the distance

ranges. The graph visualization of the same residential single family house and industrial area as in Figure 3 are shown in Figure 5 for visual comparison. Despite the overlapping of the distance range and the wider interquartile range the graph structure of the industrial area is more distinctive in the 40-150 m range while the graph of the single family house-area has a higher degree of connection in the 0-60 m range. Afterwards the graph measures are computed. The box plot of the beta index and clustering coefficient are shown in Figure 6. The interquartile range in the beta index in 0-60 m range of single family houses, allotment and center areas displayed small overlaps with the industrial and block areas. But in general a decrease of the beta index from the shorter to the longer distance range is visible for single family houses, allotment and center areas. Whereas the graph structure for industrial and block buildings shows an increase.

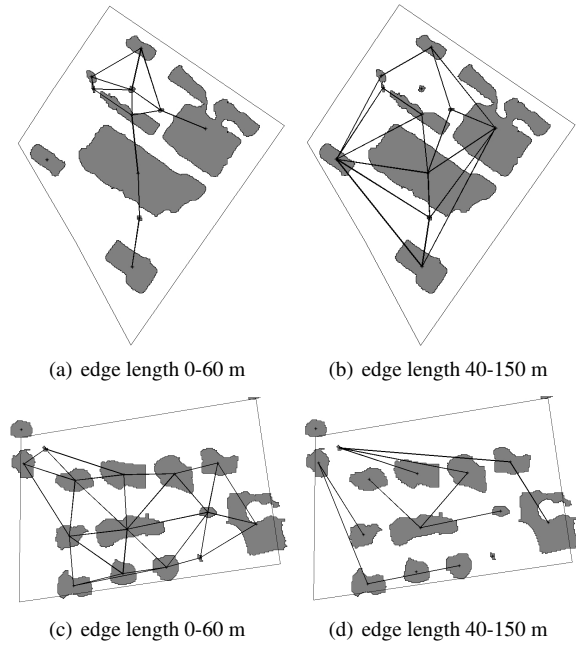


Figure 5: Planar graphs of building objects derived from the Quickbird scene: industrial area (a),(b); residential single family house-area (c),(d)

A combination of the distance classes and the computed increase or decrease can be helpful to distinguish between the two groups. This aggregation of graph measures for different spatial, relational or topological properties should result in a significant signature for each LU-class.

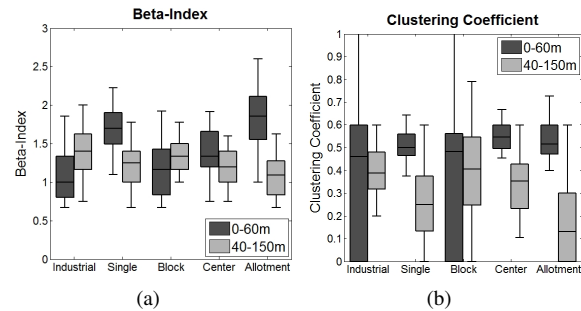


Figure 6: Box plots of beta index(a) and clustering coefficient(b) of planar graphs of building objects derived from the Quickbird scene

The box plot of the clustering coefficient do not vary much compared to the one with cadastral building polygons. The interquartile range of single family houses, allotment and center areas is

still very narrow in the shorter distance range and shows a decrease for longer distances. The clustering of industrial and block areas has a wide spread especially for shorter distances. On the basis of the clustering coefficient alone a distinction of the LU-classes is not possible.

6 CONCLUSION AND FUTURE WORK

The distribution of the cadastral building polygons as well as the building objects derived from the Quickbird image is rather dispersed or random than clustered. This fact legitimated the evaluation of the graph structure relating to different distance ranges. Particularly the beta index of the shorter distance range is a significant measure for the distinction between two groups in the cadastral building dataset (Fig. 4(a)). Better results could be achieved using the graph structures of both distance ranges and combine the results to a land use signature. Using the building land cover objects derived from the Quickbird scene a displacement of the mean distances and a widening of the interquartile ranges was observed. A reason for that is the prior merging of the segmented building polygons. This resulted predominantly in the city center in large rather than separated buildings. Also in single family house areas a merging of neighboring building objects means a fusion of the residential house with the adjacent garage, as in Fig. 5 compared to Fig. 3 is shown. A re-segmentation to generate sub-partitions of the merged building objects should be considered for future analysis. However this circumstance led to an adjustment of the distance ranges. Nevertheless the derived beta index of both distance ranges (Fig. 6(a)) indicated a decrease for the single family house, allotment and center classes from shorter to longer distances. On the contrary an increase of the beta index for industrial and block areas from shorter to longer distance ranges could be observed. The clustering coefficient has significant narrow interquartile ranges for single family house, allotment and center classes with both approaches (cf. Fig. 4(b) and Fig. 6(b)), which should be focused on in later work. Further research has to be done concerning graphs with several vertexes and edge attributes. Not only the distances as a spatial attribute but also the building heights, areas and direct neighborhood will be analyzed. The mentioned land use signature has to be developed further based on the combination of various graph properties in order to achieve a better LU-class separability. The adoption of supervised machine learning methods (e.g. random forest) will be utilized to analyze various graphs and graph measures simultaneously.

ACKNOWLEDGEMENTS

Very much acknowledged is the financial support of the ProExzellenz initiative of the "Thüringer Ministerium für Bildung, Wissenschaft und Kultur" (TMBWK).

REFERENCES

Anders, K.-H., Sester, M. and Fritsch, D., 1999. Analysis of settlement structures by graph-based clustering.

Banzhaf, E. and Höfer, R., 2008. Monitoring urban structure types as spatial indicators with cir aerial photographs for a more effective urban environmental management.

Barnsley, M. and Barr, S., 1997. Distinguishing urban land-use categories in fine spatial resolution land-cover data using a graph-based, structural pattern recognition system.

Bauer, T. and Steinnocher, K., 2001. Per-parcel land use classification in urban areas applying a rule-based technique.

Benz, U. C., Hofmann, P., Willhauck, G., Lingenfelder, I. and Heynen, M., 2004. Multi-resolution, object-oriented fuzzy analysis of remote sensing data for gis-ready information.

Breuste, J., Wächter, M. and Bauer, B. (eds), 2001. Beiträge zur umwelt- und sozialverträglichen Entwicklung von Stadtregionen. UFZ, Umweltforschungszentrum Leipzig-Halle, Projektbereich Urbane Landschaften, Leipzig.

Bundesministerium der Justiz, n.d. Verordnung über die bauliche Nutzung der Grundstücke (Baunutzungsverordnung - BauNVO): BauNVO.

Caldarelli, G., 2007. Scale-free networks: Complex webs in nature and technology. Oxford University Press, Oxford.

Cheng, P., Toutin, T., Zhang, Y. and Wood, M., 2003. Quickbird – geometric correction, path and block processing and data fusion.

de Almeida, J.-P., Morley, J. G. and Dowman, I. J., 2007. Graph theory in higher order topological analysis of urban scenes. *Computers, Environment and Urban Systems* 31(4), pp. 426–440.

Deuker, L., Bullmore, E. T., Smith, M., Christensen, S., Nathan, P. J., Rockstroh, B. and Bassett, D. S., 2009. Reproducibility of graph metrics of human brain functional networks. *NeuroImage* 47(4), pp. 1460–1468.

Di Gregorio, A., 2005. Land cover classification system software version 2: Based on the orig. software version 1. Environment and natural resources series Geo-spatial data and information, Vol. 8, rev. / edn, Rome and.

European Environment Agency, 2010. The european environment: State and outlook 2010 - Land Use.

Gunduz, C., Yener, B. and Gultekin, S. H., 2004. The cell graphs of cancer. *Bioinformatics* 20(Suppl 1), pp. i145–i151.

Newman, M. E. J., Strogatz, S. H. and Watts, D. J., 2001. Random graphs with arbitrary degree distributions and their applications. *Physical Review E*.

Richter, R., Schläpfer, D. and Müller, A., 2006. An automatic atmospheric correction algorithm for visible/nir imagery. *International Journal of Remote Sensing* 27(10), pp. 2077–2085.

Rodrigue, J.-P., Comtois, C. and Slack, B., 2009. The geography of transport systems. 2 edn, Routledge, London and New York.

Rodrigue, J.-P., 2009. The geography of transport systems, <http://people.hofstra.edu/geotrans> (15.01.2012).

Seto, K. C., Fragkias, M., Güneralp, B., Reilly, M. K. and Añel, J. A., 2011. A meta-analysis of global urban land expansion. *PLoS ONE* 6(8), pp. e23777.

Stuttgart, University, 2011. Netzwerke und Graphentheorie, <http://www.ifp.uni-stuttgart.de/lehre/vorlesungen/GIS1/Lernmodule/Netzwerk-analyse/Graphentheorie/> (15.01.2012).

Trauth, M. H., Gebbers, R. and Marwan, N., 2010. MATLAB recipes for earth sciences. 3 edn, Springer, Heidelberg [Germany] and New York.

UN Habitat, 2011. Annual report 2010.

Voltersen, M., 2011. Ableitung und Analyse der Bebauungsdichte in urbanen Räumen mittels hochauflösender Multispektraldaten und eines Stadthöhenmodells. Masterthesis, Friedrich-Schiller-Universität, Jena.

Watts, D. J. and Strogatz, S. H., 1998. Collective dynamics of 'small-world' networks. *NATURE* 393, pp. 440–442.